GEOPHYSICAL RESEARCH LETTERS, VOL. 33, L18203, doi:10.1029/2006GL026275, 2006

Headward growth of chasmata by volatile outbursts, collapse, and drainage: Evidence from Ganges chaos, Mars

J. A. P. Rodriguez,[1,2] Jeffrey Kargel,[3] David A. Crown,[2] Leslie F. Bleamaster III,[2] Kenneth L. Tanaka,[4] Victor Baker,[3] Hideaki Miyamoto,[2,5] James M. Dohm,[3] Sho Sasaki,[1] and Goro Komatsu[6]

Received 11 March 2006; revised 21 June 2006; accepted 22 June 2006; published 27 September 2006.

[1] The nature and significance of collapse processes in Capri, Eos, and Ganges Chasmata remain poorly understood. Using Ganges Chasma as a type locality, these chasmata are interpreted to be the result of clustering and assimilation of multiple chaotic terrains, which primarily formed by localized depressurization-induced or thermally-triggered dissociation of buried gas clathrate hydrates and explosive eruption of gas-saturated ground water. Such crustal destabilization could have been triggered by (1) deep fracture propagation from the Martian surface, (2) magmatic intrusions and associated heating and inflation-induced terrain fracturing, and/or (3) climatic thaw and thinning/weakening of the permafrost over the clathrate and gas-rich groundwater zones. Volume increases associated with release of gases contributed to the expulsion of groundwater and fluidized sediments at the surface, thereby carving the higher outflow channels peripheral to the chasmata and the lower outflow channel floors of the chasmata and outflow channels.
Citation: Rodriguez, J. A. P., J. Kargel, D. A. Crown, L. F. Bleamaster III, K. L. Tanaka, V. Baker, H. Miyamoto, J. M. Dohm, S. Sasaki, and G. Komatsu (2006), Headward growth of chasmata by volatile outbursts, collapse, and drainage: Evidence from Ganges chaos, Mars, *Geophys. Res. Lett.*, *33*, L18203, doi:10.1029/2006GL026275.

1. Introduction

[2] Capri, Eos, and Ganges Chasmata form trough systems interconnected to the east with the chaotic terrains and outflow channels of the southern circum-Chryse region of Mars [*Sharp*, 1973]. In this work, these regions are referred to as the eastern chasmata and the outflow channel regions, respectively (Figure 1). While chaotic terrains and surface flow features [*McCauley et al.*, 1972] are widespread within both the outflow channel and eastern chasmata regions, they are generally absent in the rest of Valles Marineris [*Lucchitta et al.*, 1994]. The formation of chaotic terrain has typically been attributed to voluminous emanations of fluids and/or fluidized sediments and associated ground collapse, resulting in the incisement of the outflow channels during the Late Hesperian Epoch [e.g., *Baker and Milton*, 1974; *Baker*, 1982; *Carr*, 1979; *Rodriguez et al.*, 2005]. Using Viking topographic data, *Rotto and Tanaka* [1995] discovered two main topographic levels of outflow channel floor materials: a higher floor level, which formed during the early to intermediate stages of Late Hesperian flooding, and a lower floor level, which was interpreted to have formed during the latest stages of outflow activity.

[3] Chaotic terrains in the eastern chasmata and the outflow channel regions are geomorphologically distinct, and the specific nature of collapse processes in the eastern chasmata, their volatile release history, and their role in the formation of the outflow channels, are issues that remain poorly understood to date. In this work, we seek to explain: (1) the specific nature of collapse processes in the eastern chasmata, particularly in Ganges Chasma where the deepest known chaotic terrain on Mars, the Ganges chaos, is located (Figures 1 and 2); and (2), the volatile release history related to collapse processes in the eastern chasmata, particularly in relation to the lower outflow channel floors, the source regions of which have not been clearly identified.

2. Morphology and Morphometry of Ganges Chaos

[4] Ganges chaos (Figures 1 and 2) is a north-trending, alcove-shaped depression situated along the southern margin of Ganges Chasma. It is approximately 90 km wide and 120 km long, and its cavity volume is $\sim$29,300 km^3. MOLA topography reveals that the floor of Ganges chaos consists of three cells, two of which are enclosed and contain chaotic materials (1 and 2 in Figure 2b). The other opens northward into the floor of Ganges Chasma and exhibits only traces of chaotic terrain (3 in Figure 2b). Important geomorphic differences between Ganges chaos and the chaotic terrains in the outflow channel region include: (1) the maximum rim-to-floor depth of Ganges chaos is 6 km, whereas for other chaos in the outflow channel region it is about 2 km; (2) Ganges chaos consists of large and densely fractured mesas that preserve plateau surfaces (Figures 2c, 3, and 4a), whereas the outflow channel region primarily consists of plateau materials highly disrupted into knobby materials [*Carr*, 1979]; and (3) the plateau surfaces that form the margins of the eastern chasmata region lack the crustal subsidence features characteristic of the degraded geologic terrain that forms

[1]National Astronomical Observatory, Mizusawa, Japan.
[2]Planetary Science Institute, Tucson, Arizona, USA.
[3]Department of Hydrology and Water Resources, University of Arizona, Tucson, Arizona, USA.
[4]Astrogeology Team, U.S. Geological Survey, Flagstaff, Arizona, USA.
[5]Department of Geosystem Engineering, University of Tokyo, Tokyo, Japan.
[6]International Research School of Planetary Sciences, Pescara, Italy.

0094-8276/06/2006GL026275$05.00

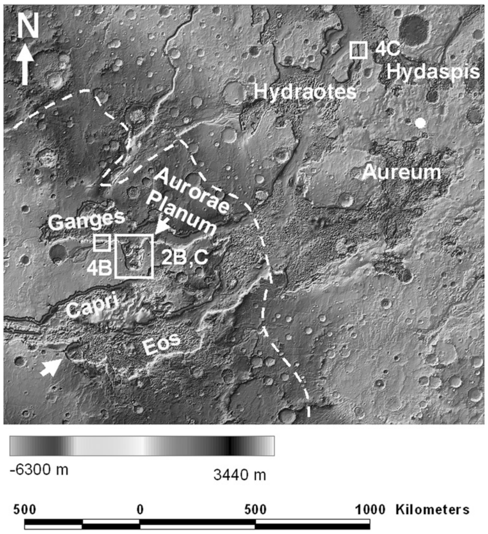

Figure 1. MOLA DEM showing the eastern chasmata and outflow channel regions (zones respectively west and east of the dashed white line, [55.270E, 7.447N to 23.699E, 20.094S]), Figure panels 2b, 2c, 4b, and 4c are shown. The Eos, Capri and Ganges Chasmata, and the Hydraotes, Aureum and Hydaspis chaotic terrains are identified. The white dot shows the location of subsided plateau surfaces that form the margins of the Aureum, Hydraotes and Hydaspis chaotic terrains.

the margins of the chaotic terrains in the outflow channel region [*Rodriguez et al.*, 2005] (see white dots in Figures 1 and 2a).

[5] Unlike in the outflow channel region, higher outflow channel activity in Aurorae Planum (as well as in the rest of the eastern chasmata region) did not result in multiple levels of incised canyons interconnecting the higher and lower channel floor systems (Figure 4b), and the channels source from discrete chaotic terrains and pits, the margins of which show no evidence of crustal subsidence (e.g., black arrows in Figure 2a). These observations suggest that higher outflow channel activity resulted from localized depletion of crustal volatiles and that surface flow was not sustained long enough to deeply incise the plateau materials, possibly due to the relatively short duration of these floods.

3. Formation of Ganges Chaos

[6] The existence of chaotic terrains and outflow channels in the eastern chasmata indicates that the regional upper crust must have been volatile enriched. Other regions of Mars that may consist of volatile-enriched crustal materials display creep-like features [*Lucchitta*, 1984; *Kargel*, 2004; *Crown et al.*, 2005] and/or extensive plateau surface warping [e.g., *Rodriguez et al.*, 2005]. On the other hand, steep scarps bound the eastern chasmata systems, including the individual cells comprising Ganges chaos, which indicates that the plateau materials are mechanically robust. The margins of Ganges Chasma display various alcove-like reentrants, which contain chaotic terrains. One of these forms the west end of Ganges Chasma and is similar in shape and dimensions to Ganges chaos but better resembles the remainder of the chasma due to its deep floor. Two others resemble Ganges chaos' individual cells (white arrows in Figure 2a). Similarly, Eos Chasma displays alcove-like margins, one of which forms a semi-enclosed pit (lower left white arrow in Figure 1). The cell-like nature of these chaotic terrains suggests that the growth of the eastern chasmata involved the nucleation and amalgamation of numerous subsurface cavities, and that multiple events of outflow activity and collapse led to the formation of coalesced clusters of the trough systems that form the eastern chasmata.

3.1. Geothermal Formation of a Gas-Rich Sub-Permafrost Aquifer

[7] Figure 5 shows that liquid CO_2 and CO_2-saturated liquid water could have been stable under an impermeable cap, presumably ice- or salt-cemented rock, under conditions that did not require extraordinary levels of geothermal heat or climate warming [*Kargel*, 2004; *Hoffman*, 2000]. Whereas climate/geothermal warming [*Kargel*, 2004; *Kargel et al.*, 2006] or tectonic rupturing of the permafrost may have yielded conditions, perhaps the trigger, for this rapid sequence of events, the endothermic nature of clathrate dissociation means that to have fluid volume

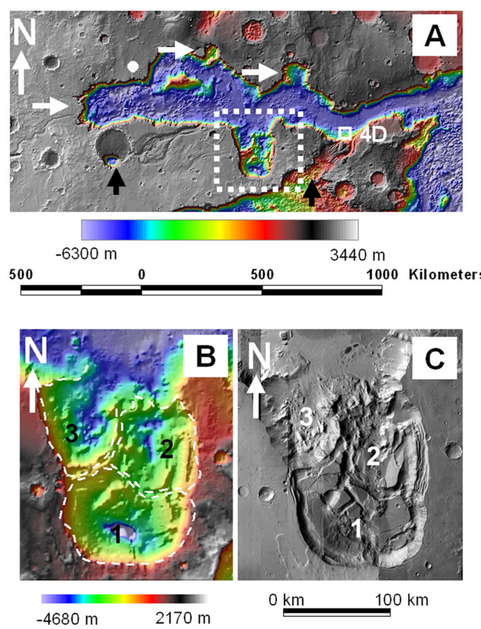

Figure 2. (a) MOLA DEM of Ganges Chasma centered at [46.651 E, 8.009 S]. Panel for Figure 4d is shown. The dashed square shows the location of Figures 2b and 2c. The black arrows show the locations of higher outflow channels in Aurorae Planum. The white arrows show the other alcove-like depressions of various dimensions along the margin Ganges Chasma. The white dot shows the plateau surface that forms the margins of Ganges Chasma, which in contrast with those around the chaotic terrains in the outflow channel region, does not display evidence for surface subsidence. (b) MOLA DEM of Ganges chaos. The floor of Ganges chaos consists of three cells numbered 1 to 3. (c) THEMIS IR mosaic of Ganges chaos. The chaotic terrain within the cells 1 and 2 primarily consists of densely fractured blocks of subsided plateau materials. Cell 3 opens into the chasma floor and lacks chaotic material.

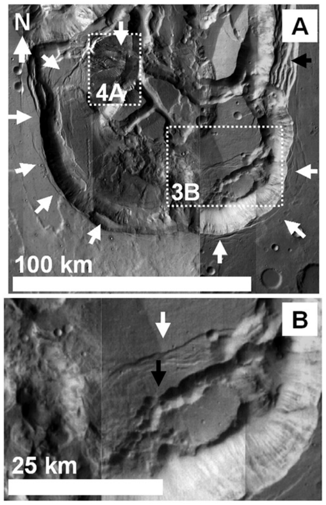

Figure 3. (a) THEMIS IR mosaic of cell 1 within the Ganges chaos. The plateau margins around this depression, and the large mesas within it, display dense systems of extensional faults arranged concentric to the center of the depression (white arrows). The black arrow shows part of the eastern margin of cell 2. Notice how closely spaced faults modify the margin of the plateau. Boxes show locations for Figures 3b and 4a. (b) The white arrow shows the location of a densely fractured graben floor of a mesa within cell 2. The black arrow shows a parallel trough that passes SW into a pit chain.

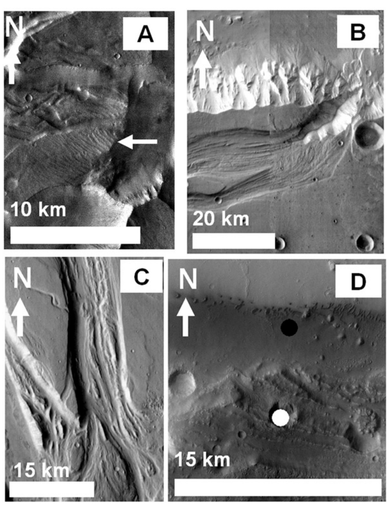

Figure 4. (a) Subframe of THEMIS VIS V06219001 showing scoured surfaces of highly fractured blocks within Ganges chaos (white arrow). (b) THEMIS IR mosaic. Higher outflow channel floor on the Aurorae Planum plateau surface that forms the southern margin of Ganges Chasma. (c) Subframe of THEMIS I02123002. Higher outflow channel floor proximal to Hydaspis Chaos in the outflow channel region characterized by multiple topographic levels of entrenched canyons with floors as deep as the adjacent lower outflow channel floor. (d) Subframe of THEMIS V10550001. Remnant of a highly scoured channel floor in Ganges Chasma (white dot), and adjacent lower outflow channel floor (black dot).

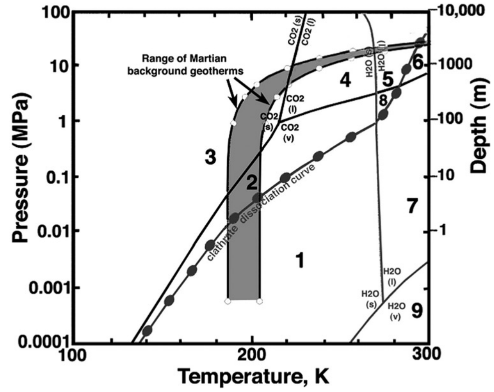

Figure 5. Modeled Martian geotherms are superposed on the principal phase fields in the system H_2O-CO_2. A range of thermal conduction profiles were calculated for (1) basalt thermal conductivity; (2) global mean heat flow calculated for 3.5 billion years ago (scaled from Earth's modern heat flow using planetary mass and surface area, and scaled using radioactive decay constants for major long-lived radioisotopes); and (3) a range of low-latitude mean annual surface temperatures 3.5 billion years ago (scaled from today's equatorial temperatures with 25% lower solar luminosity and no albedo difference). Principal phase fields are numbered; the most important for our work are the fields numbered (3) clathrate + either water ice or dry ice (whichever is in excess relative to the stoichiometry of cage-filled Type 1 CO_2 clathrate); (4) clathrate + either liquid CO_2 or ice (whichever is in excess); (5) clathrate + either liquid CO_2 or liquid H_2O containing dissolved CO_2; (6) liquid water containing CO_2, and immiscible liquid CO_2 containing dissolved water. The geotherms would encounter either (a) liquid CO_2 at a depth of about 700 m if there is excess CO_2, and a 2-liquid zone (gas-saturated liquid water, and water-saturated liquid CO_2) upon clathrate dissociation at about 2400 m depth; or (b) gas-saturated water at a depth of 1700 m and two liquids at 2400 m due to clathrate dissociation. Phase diagram after *Longhi* [2000] and *Kargel* [2004].

sufficient to initiate an explosive expulsion of material, much of the volatile mass was already in fluid form at the time of the events. An impermeable lid is needed to confine these volatiles; permafrost ice or salts could provide the sealant. Methane clathrate systems would exhibit similar behavior, though phase boundaries are shifted.

3.2. A Model for Tectonically Induced Nucleation of Subsurface Cavities, Collapse and Outflow Activity

[8] We propose that a frozen layer above the liquid CO_2 transition acted as a brittle lid (Figure 5), and that impacts, thinning and weakening of the permafrost due to climatic warming or slight increases in the geothermal conditions, may have fractured the lid resulting in a series of runaway degassing events.

[9] Depressurization-driven rapid volatile exsolution within zones 4, 5 and 6 in Figure 5, and associated volumetric expansion [*Komatsu et al.*, 2000; *Baker et al.*, 1991] would result in the migration of volatiles and

entrained clastic material along faults to the Martian surface, producing geyser eruptions and volatile discharges onto Aurorae Planum and possibly onto the adjacent chasma floor. The apparent erosion of densely faulted grabens into pit chains and troughs (e.g., Figure 3b), and the existence of scoured channel floor remnants including the scoured surfaces shown in Figures 4a and 4d are consistent with this scenario. The plateau surfaces around Ganges chaos do not display outflow channel floors, indicating that the channel materials within Ganges chaos were produced by floods that emerged locally.

[10] Sustained removal of subsurface volatiles would initiate regional subsidence, which would in turn generate dense systems of normal faults produced by extensional deformation of the brittle upper crustal zone [*Rodriguez et al.*, 2005], as indicated by the systems of grabens and fissures marking the periphery of Ganges chaos, as well as the surfaces of blocks and mesas within it (Figures 2c and 4a). The floors and margins of the grabens that separate the grooved mesas that form channel floor remnants within Ganges chaos are not marked by flow features (Figure 4a), which indicates that ground rupture and chaos formation post-dated outflow activity.

[11] Normal faults are arranged concentrically to the center of Ganges chaos cells 1 and 2 (Figures 2c and 3a). Subsurface fault convergence led to the rapid depressurization of the crustal materials under the subsiding brittle lid. Resultant explosive H_2O-CO_2 effervescence and accelerated clathrate dissociation led to the liquefaction of poorly consolidated, thawed parts of the crust [*Bernt et al.*, 2004] underlying the lid to a maximum depth of 5 km. Liquefaction was autocatalytic in the sense that fracturing and fluidized rock and volatile expulsion led to (a) continued undermining and fracturing of the terrain, (b) accelerating depressurization, (c) fractional and gravitational heating of the rocks, and (d) expansion of conduits needed for sustained expulsion of materials. Nevertheless, the endothermic properties of clathrate dissociation would cool down the cellular domain of crustal disintegration and result in a reduction of gas content in the aquifer. Factors which would limit the crustal volume of liquefaction [*Bernt et al.*, 2004], perhaps to one cell size (10^4 km^3), which is consistent with the apparent chasmata formation and growth by subsurface cavity nucleation and amalgamation.

[12] Rapid subsidence of the lithified or frozen lid helped to sustain high hydraulic pressure and cause dynamic rearrangement of the internal stress fields within the aquifer system, thus driving crustal fragmentation and high hydraulic head along the southern margin of Ganges Chasma. Expansion of the liquefaction zone thinned the walls separating the aquifer from the floor of Ganges Chasma, leading to wall failure and evacuation of liquefied geologic materials in pulses of giant debris flows, which is consistent with the fact that Ganges chaos cell 3 opens to the north into the floor of Ganges Chasma, contains only traces of chaotic materials and no subsided fractured blocks (3 in Figure 2b), which indicates that large amounts of crustal materials were expulsed onto a pre-existing Ganges Chasma floor. These debris flows excavated the lower parts of the lower outflow channel floors in Ganges Chasma, and destroyed pre-existing channel floor materials (Figure 4d).

[13] The general absence of Ganges chaos-like chaotic terrain within the eastern chasmata indicates that the bulk of the collapsed plateau materials were effectively displaced from the chasmata, most likely by density flows. Thus, we conclude that the lower outflow channels that form the base of dissection in the eastern chasmata and outflow channel regions [*Scott and Tanaka*, 1986; *Rotto and Tanaka*, 1995] were carved by debris flows ensued by catastrophic discharges within the eastern chasmata region [e.g., *Tanaka et al.*, 2001].

[14] **Acknowledgments.** We give credit to Dr. Philip Christensen, at Arizona State University, for the elaboration of the THEMIS data release website (http://themis.asu.edu/), and to the MOLA team.

References

Baker, V. R. (1982), *The Channels of Mars*, Univ. of Texas Press, Austin.
Baker, V. R., and D. J. Milton (1974), Erosion by catastrophic floods on Mars and Earth, *Icarus*, *23*, 27–41.
Baker, V. R., R. G. Strom, V. C. Gulick, J. S. Kargel, G. Komatsu, and V. S. Kale (1991), Ancient oceans, ice sheets and the hydrological cycle on Mars, *Nature*, *352*, 589–594.
Bernt, C., J. Mienert, M. Vanneste, and S. Bünz (2004), Gas hydrate dissociation and seafloor collapse in the wake of the Storegga Slide, Norway, in *Onshore-Offshore Relationships on the North Atlantic Margin*, *NPF Spec. Publ.*, edited by B. T. G. Wandås et al., pp. 285–292, Elsevier, New York.
Carr, M. H. (1979), Formation of Martian flood features by release of water from confined aquifers, *J. Geophys. Res.*, *84*, 2995–3007.
Crown, D. A., L. F. Bleamaster III, and S. C. Mest (2005), Styles and timing of volatile-driven activity in the eastern Hellas region of Mars, *J. Geophys. Res.*, *110*, E12S22, doi:10.1029/2005JE002496.
Hoffman, N. (2000), White Mars: A new model for Mars' surface and atmosphere based on CO_2, *Icarus*, *146*, 326–342.
Kargel, J. S. (2004), *Mars: A Warmer, Wetter Planet*, 557 pp., Springer, New York.
Kargel, J. S., J. E. Begét, R. Wessels, and J. E. Skinner Jr. (2006), "Bottom-up" geothermal interactions and "top-down" climatic interactions with permafrost and hydrates on Mars, *Lunar Planet. Sci. XXXVII*, abstract 2308.
Komatsu, G., J. S. Kargel, V. R. Baker, R. G. Strom, G. G. Ori, C. Mosangini, and K. L. Tanaka (2000), A chaotic terrain formation hypothesis: Explosive outgas and outflow by dissociation of clathrate on Mars, *Lunar Planet. Sci. Conf.*, *XXXI*, abstract 1434.
Longhi, J. (2000), Low-temperature phase relations in the CO_2-H_2O system with application to Mars, *Lunar Planet. Sci. Conf.*, *XXXI*, abstract 1518.
Lucchitta, B. K. (1984), Ice and debris in the fretted terrain, Mars, *J. Geophys. Res.*, *89*, Suppl., B409–B418.
Lucchitta, B. K., N. K. Isbell, and A. Howington-Kraus (1994), Topography of Valles Marineris: Implications for erosional and structural history, *J. Geophys. Res.*, *99*, 3783–3798.
McCauley, J. F., M. H. Carr, J. A. Cutts, W. K. Hartmann, H. Masursky, D. J. Milton, R. P. Sharp, and D. E. Wilhelms (1972), Preliminary Mariner 9 report on the geology of Mars, *Icarus*, *17*, 289–327.
Rodriguez, J. A. P., S. Sasaki, R. O. Kuzmin, J. M. Dohm, K. L. Tanaka, H. Miyamoto, K. Kurita, G. Komatsu, A. G. Fairén, and J. C. Ferris (2005), Outflow channel sources, reactivation and chaos formation, Xanthe Terra, Mars, *Icarus*, *175*, 36–57.
Rotto, S., and K. L. Tanaka (1995), Geologic/geomorphic map of the Chryse Planitia Region of Mars, 1:5000,000, *U.S. Geol. Surv. Misc. Invest. Map*, *I-2441-A*.
Scott, D. H., and K. L. Tanaka (1986), Geologic map of the western equatorial region of Mars, *U.S. Geol. Surv. Misc. Invest Map*, *I-1802-A*, 1:15,000,000.
Sharp, R. P. (1973), Mars: Troughed terrain, *J. Geophys. Res.*, *78*, 4063–4072.
Tanaka, K. L., W. B. Banerdt, J. S. Kargel, and N. Hoffmann (2001), Huge, CO_2-charged debris-flow deposit and tectonic sagging in the northern plains of Mars, *Geology*, *29*, 427–430.

V. Baker, J. M. Dohm, and J. Kargel, Department of Hydrology and Water Resources, University of Arizona, Tucson, AZ 85721, USA.

L. F. Bleamaster III and D. A. Crown, Planetary Science Institute, Tucson, AZ 85719, USA.

H. Miyamoto, Department of Geosystem Engineering, University of Tokyo, Tokyo 113-8656, Japan.

K. L. Tanaka, Astrogeology Team, U.S. Geological Survey, Flagstaff, AZ 86001, USA.

G. Komatsu, International Research School of Planetary Sciences, I-65127 Pescara, Italy.

J. A. P. Rodriguez, Planetary Science Institute, 1700 E Ft. Lowell, Suite 106, Tucson, AZ 85719, USA. (alexis@psi.edu)

S. Sasaki, National Astronomical Observatory, Mizusawa 023-0861, Japan.